Supplementary for

Impacts of Complex Terrain Features on Local Wind Field and $PM_{2.5}$ Concentration

Yuqiang Song [1] and Min Shao [2,*]

[1] Dalian Meteorological Observatory, Dalian 116000, China
[2] School of Environment, Nanjing Normal University, Nanjing 210046, China
* Correspondence: mshao@masonlive.gmu.edu

Text S1 The impacts of Mt. LS and the Yangtze River on PM2.5 transport

Figure S1 and Figure S2 are cases that $PM_{2.5}$ transportations were obviously affected by terrain features (22:00 LST on January 10th to 00:00 LST on January 11th, 2019 for Mt. LS, and from 22:00 LST on April 3rd to 2:00 on April 4th, 2019 for the Yangtze River).

As shown in Fig. S1, before Mt. LS is "removed" (CTRL_HGY, CTRL_QX, CTRL_GL), the transport of $PM_{2.5}$ is affected by the wind field and transported southwest along the southeast side of Mt. LS, and tends to be blocked by Mt. LS. The transport of $PM_{2.5}$ in experiments CTRL_HGY and CTRL_QX is more obvious. In experiment CTRL_GL, the transport of $PM_{2.5}$ across the Yangtze River is blocked by Mt. LS and then move towards southwest. After Mt. LS is "removed", the concentration of $PM_{2.5}$ in Mt. LS direction of different experiments increases by about 0.2-0.3ug/m3, which is about 20% higher than those CTRL experiments.

As shown in Fig. S2, before the "removal" of the Yangtze River (CTRL_QX, CTRL_GL), $PM_{2.5}$ is basically transported from the point sources to the east, and is blocked by Mt. LS after crossing the Yangtze River. The concentration of $PM_{2.5}$ decreases obviously when reaching Mt. LS, and tends to transport to the southwest, but this tendency is not obvious. After the Yangtze River is "removed" (YZR_QX, YZR_GL), the transport of $PM_{2.5}$ to the west is weakened, thus leading to a decrease in $PM_{2.5}$ concentration. However, in the experiment YZR_QX, the concentration of $PM_{2.5}$ increases at the south of Baguazhou where the Yangtze River splits, which is related to the enhanced east wind in this area. In experiment YZR_GL, the concentration of $PM_{2.5}$ also increases in a small area over the Yangtze River, which may be caused by the weakening of the transport ability of $PM_{2.5}$ across the river after the Yangtze River is "removed". During other periods, such topographic effects are similar to those in Fig. S1 and Fig. S2 when the background wind field is dominated by east or northeast wind, which will not be elaborated on here.

Text S2 Comparisons of simulated and observed wind direction from different experiments

Figure S3 is the comparisons of simulated and observed wind direction from different experiments at Pukou Station. Comparing Figure S3.a and Figure S3.b, by improving the resolution of WRF from 1000 m to 300 m, the wind simulations are significantly improved. The Abias of WRF are reduced by 27°-68° and the Abias of CALMET are reduced by 25°-71°. The RMSEs of WRF are reduced 39°-103° and the RMSE of CALMET are reduced 40°-103°. These results indicate that the finer resolution of WRF could greatly improve wind simulation both in WRF and CALMET. Comparing Figure S3.b and Figure S3.c, the Abias of CALMET were reduced by 5°-8° and the RMSEs were reduced by 5°-8°after updating landuse. From the above analysis, we could achieve that increasing the resolution of WRF will significantly improve the wind field simulation, which can be further improved by upgrading the landuse data.

Text S3 The $PM_{2.5}$ concentration and wind differences between WRF1000_CALMET1000 and WRF300_CALMET150_LU from experiments with three different virtual emission point sources

As shown in Figure S4, WRF1000 was used as the meteorological first guesses, and the horizontal resolution of CALMET was set to 1000m for wind field diagnosis. Then, the wind field diagnosis results and the three virtual point sources are used to simulate the diffusion of PM2.5. Finally, the WRF_CALMET150_LU results were interpolated to the grid of WRF1000_CALMET1000, and the analysis are shown in Figure S4. Figure S4 shows that the north wind is strengthened in January and the south wind is strengthened in other months from the results of WRF1000_CALMET1000. This is probably due to the weakened terrain drag effects due to coarser grid resolutions. The differences of PM2.5 concentration mainly occur in the downwind direction of the point sources. But it needs to be emphasized that using the coarser meteorological and terrain data will bring some variations, so higher precision simulations are recommended.

Text S4 comparisons of simulated and observed wind from different experiments at Liuhe Station

As shown in Table S1, after improving the resolution of WRF from 1000 m to 300 m, the Bias and RMSE of WRF and CALMET didn't change significantly and the correlation coefficient decreased indeed.

In the comparisons of simulated and observed wind direction from different experiments (Table S2), after improving the resolution of WRF, the Abias and RMSEs of WRF results were improved by around 30° in July and October, but degrades were found in other months. The Abias and RMSEs of WRF results were increased by 0-12°, which change slightly between WRF300_CALMET150 and WRF300_CALMET150_LU.

The simulated wind direction didn't improve in these groups of experiments, this is because it involves the simulation of small scale turbulence. For a mesoscale simulation, to represent the turbulence state in the boundary layer, a boundary layer parameterization scheme is usually used to represent the average state within a certain scale, whose applicable theoretical resolution is greater than 1 km. As we continue to improve the resolution, similar problems would occur.

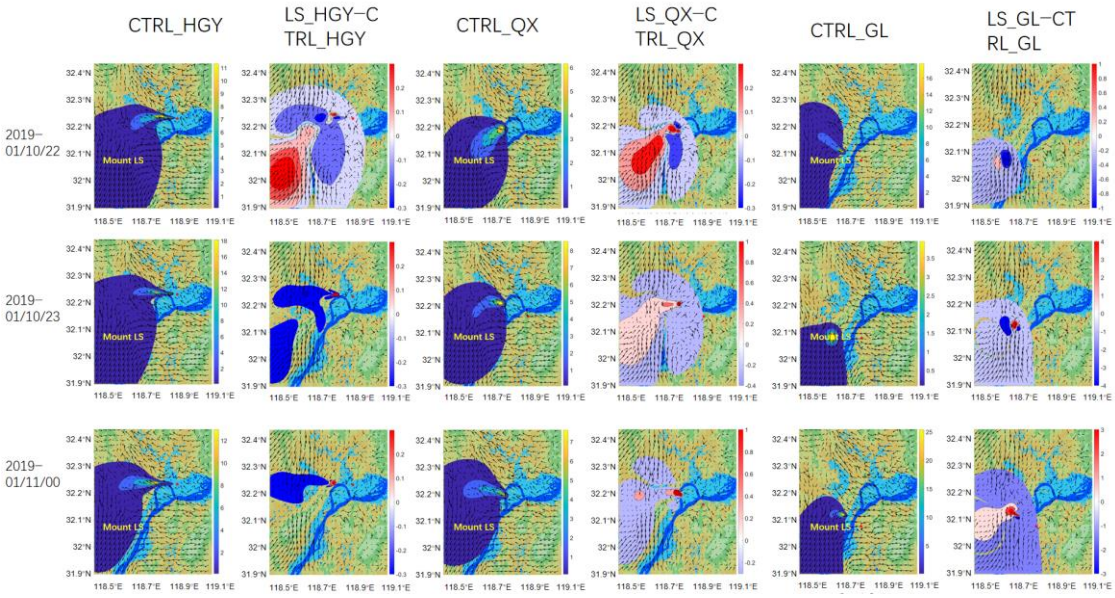

Figure S1. Spatial distributions of $PM_{2.5}$ concentrations and the differences between before and after Mount. LS is "removed" from experiments with different point sources (ug/m^3).

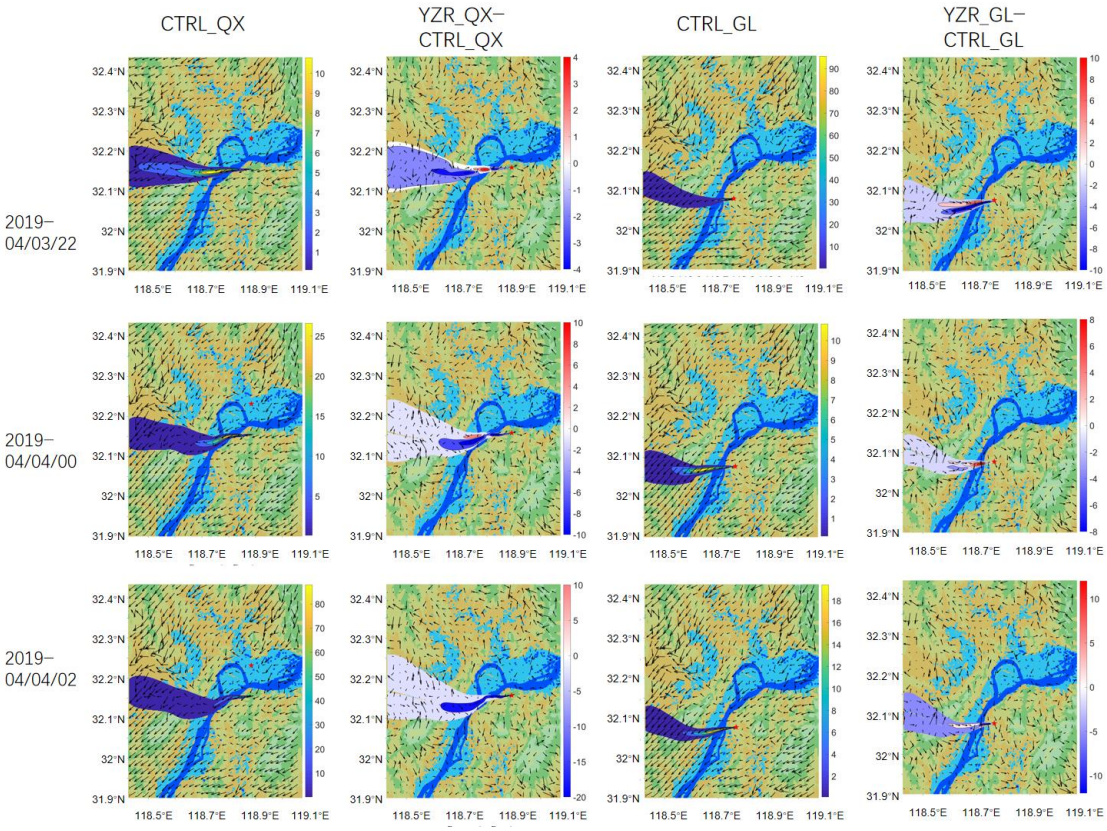

Figure S2. Similar to Figure S1, but for the "removal" of the Yangtze River.

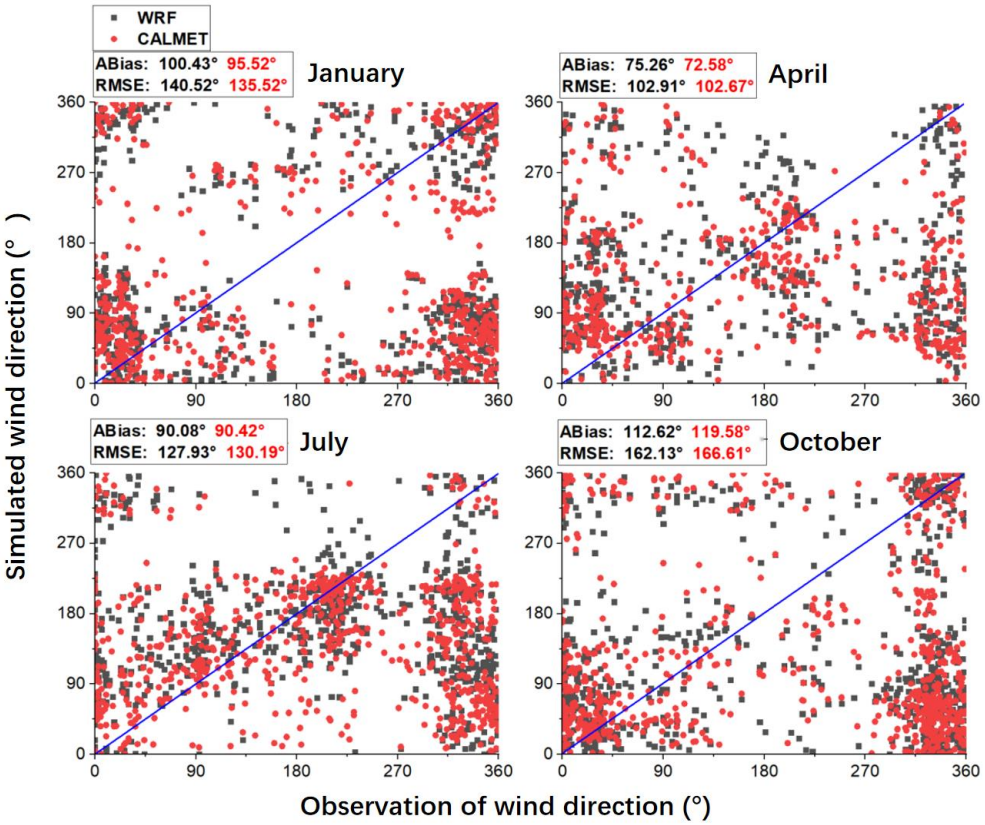
WRF
CALMET
ABias: 100.43° 95.52°
RMSE: 140.52° 135.52°
January
ABias: 75.26° 72.58°
RMSE: 102.91° 102.67°
April
ABias: 90.08° 90.42°
RMSE: 127.93° 130.19°
July
ABias: 112.62° 119.58°
RMSE: 162.13° 166.61°
October
Simulated wind direction (°)
Observation of wind direction (°)

(a)

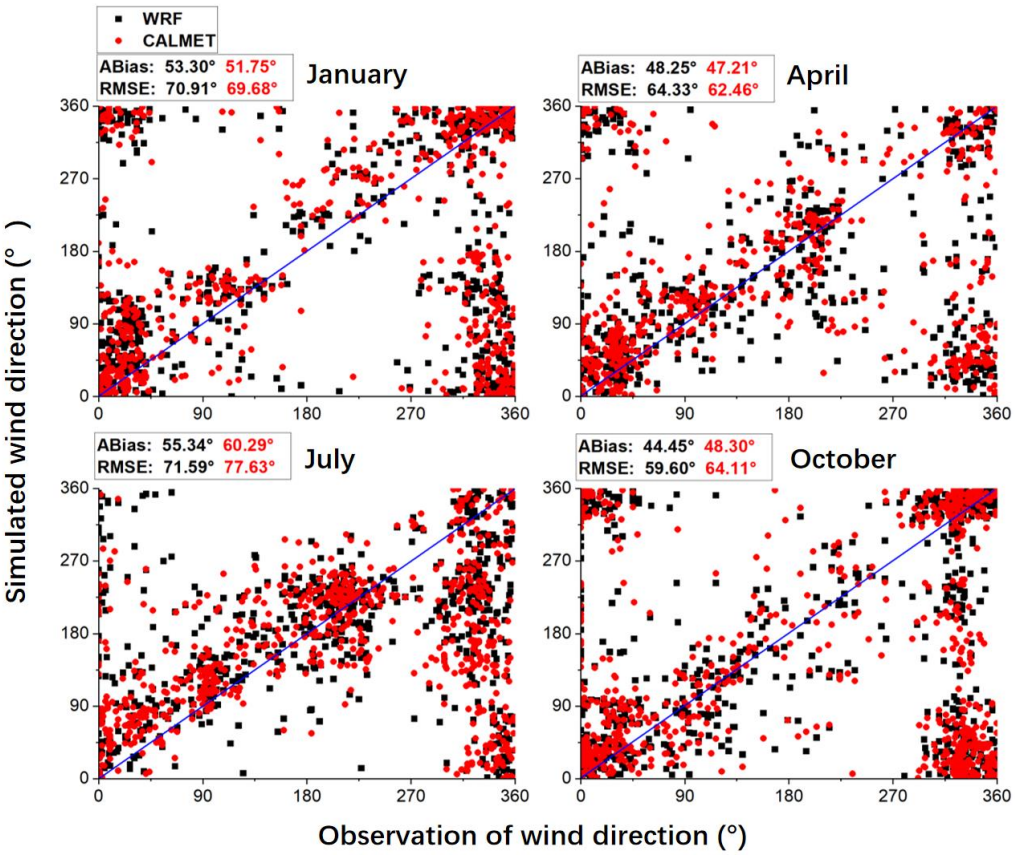
WRF
CALMET
ABias: 53.30° 51.75°
RMSE: 70.91° 69.68°
January
ABias: 48.25° 47.21°
RMSE: 64.33° 62.46°
April
ABias: 55.34° 60.29°
RMSE: 71.59° 77.63°
July
ABias: 44.45° 48.30°
RMSE: 59.60° 64.11°
October
Simulated wind direction (°)
Observation of wind direction (°)

(b)

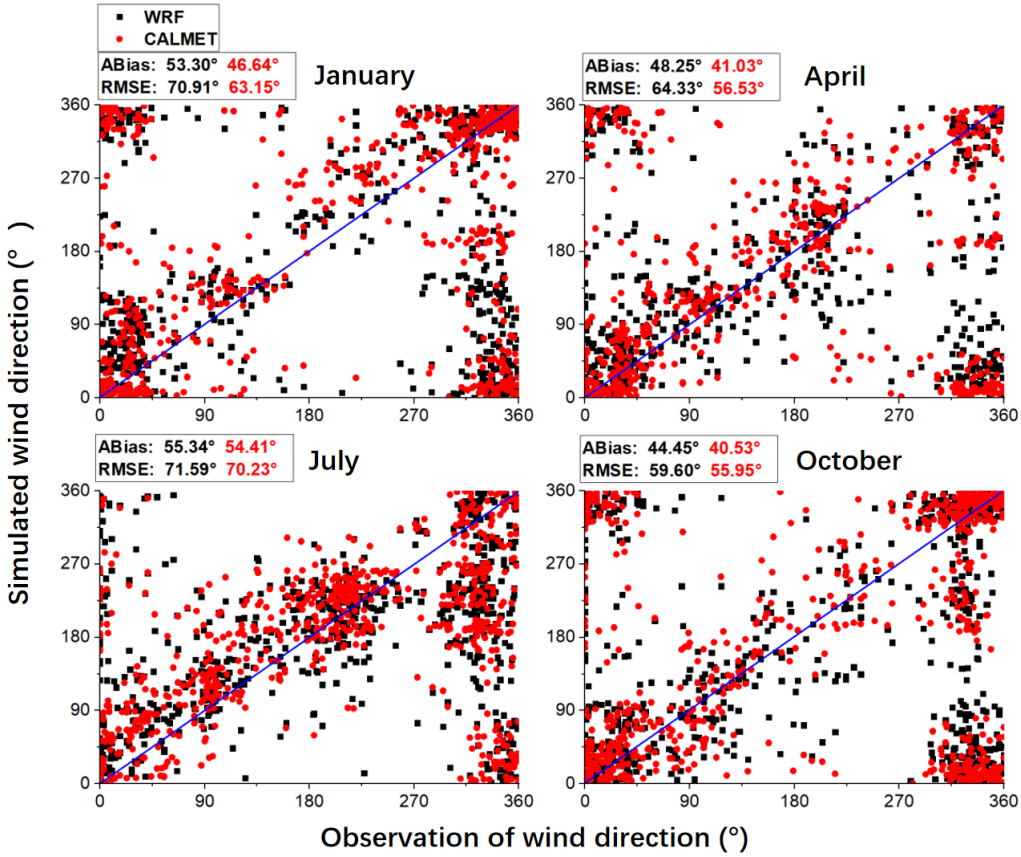

(c)

Figure S3. Comparisons of simulated and observed wind direction from different experiments: (a) WRF1000_CALMET150; (b) WRF300_CALMET150; (c) WRF300_CALMET150_LU.

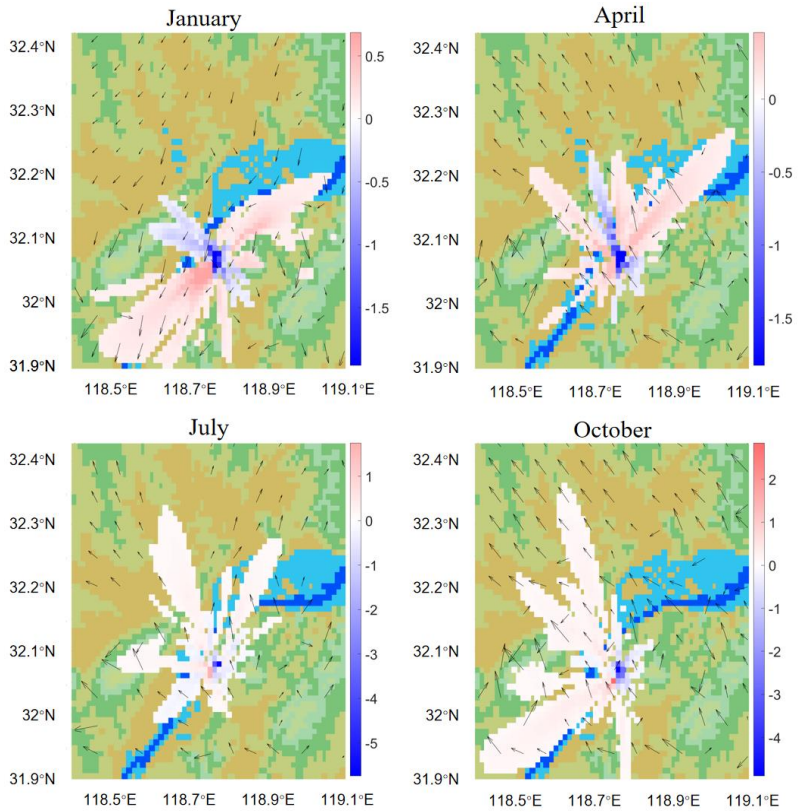
January
April
July
October
32.4°N
32.3°N
32.2°N
32.1°N
32°N
31.9°N
118.5°E
118.7°E
118.9°E
119.1°E
0.5
0
-0.5
-1
-1.5
0
-0.5
-1
-1.5
1
0
-1
-2
-3
-4
-5
2
1
0
-1
-2
-3
-4

(a)

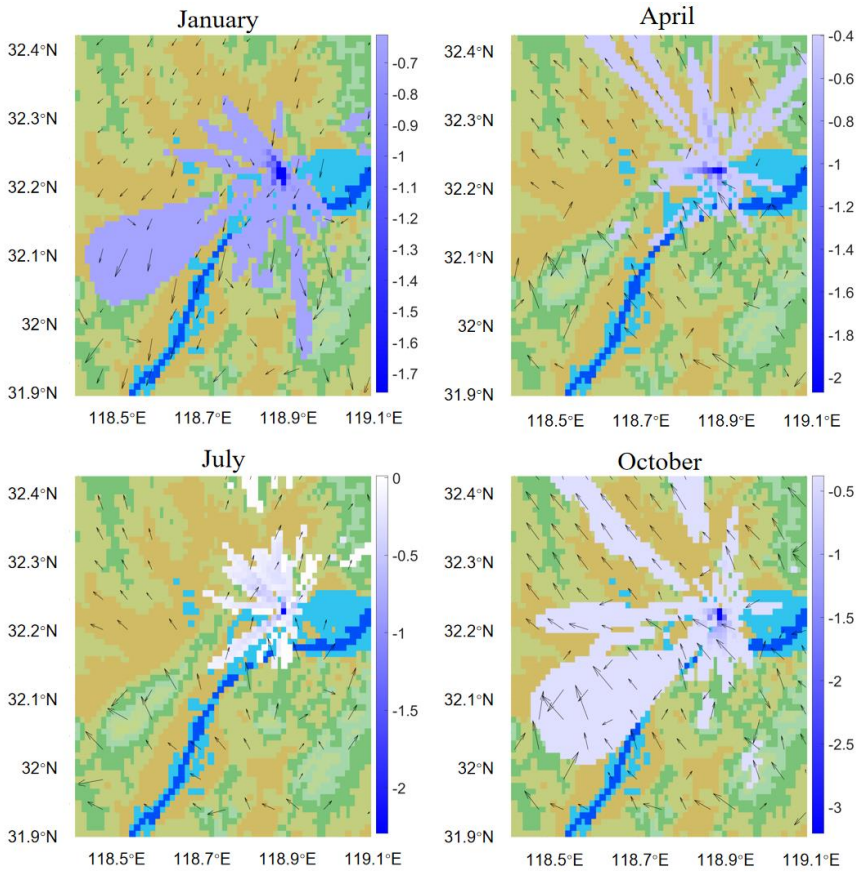
January
April
July
October
32.4°N
32.3°N
32.2°N
32.1°N
32°N
31.9°N
118.5°E
118.7°E
118.9°E
119.1°E
-0.7
-0.8
-0.9
-1
-1.1
-1.2
-1.3
-1.4
-1.5
-1.6
-1.7
-0.4
-0.6
-0.8
-1
-1.2
-1.4
-1.6
-1.8
-2
0
-0.5
-1
-1.5
-2
-0.5
-1
-1.5
-2
-2.5
-3

(b)

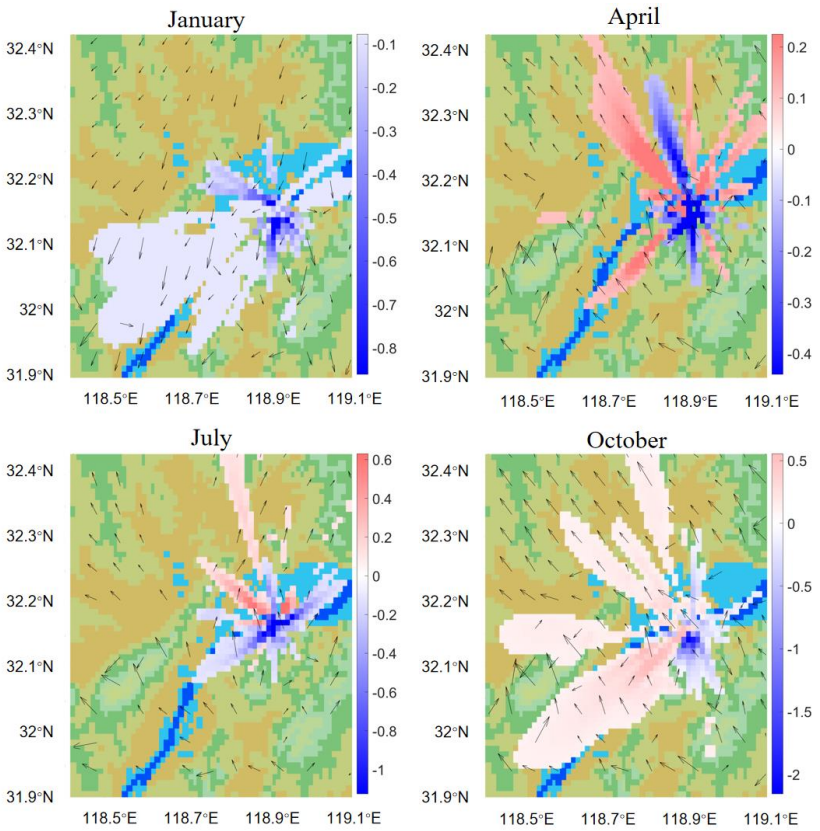

(c)

Figure S4. The $PM_{2.5}$ concentration and wind differences between WRF1000_CALMET1000 and WRF300_CALMET150_LU from experiments with three different virtual emission point sources (ug/m^3): (a) Gulou District; (b) Jiangbei Chemical Industry Park; (c) Qixia District.

Table S1. Verified wind speed of Liuhe Station.

		WRF1000_CALMET150		**WRF300_CALMET150**		**WRF300_CALMET150_LU**	
		WRF	CALMET	WRF	CALMET	WRF	CALMET
January	Bias	1.41	1.09	1.04	0.85	1.04	0.85
	RMSE	3.39	2.20	3.09	2.36	3.09	2.36
	R	0.59	0.66	0.34	0.38	0.34	0.38
April	Bias	1.42	0.91	1.11	0.83	1.11	0.83
	RMSE	3.77	2.12	3.85	2.72	3.85	2.72
	R	0.63	0.68	0.47	0.49	0.47	0.49
July	Bias	0.12	0.69	0.83	0.64	0.83	0.64
	RMSE	2.93	1.52	2.56	1.84	2.56	1.84
	R	0.29	0.58	0.47	0.52	0.47	0.52
October	Bias	0.92	1.29	1.29	1.15	1.29	1.15
	RMSE	3.24	2.68	3.28	2.67	3.28	2.68
	R	0.64	0.69	0.51	0.54	0.51	0.54

Table S2. Verified wind direction of Liuhe Station.

		WRF1000_CALMET150		**WRF300_CALMET150**		**WRF300_CALMET150_LU**	
		WRF	CALMET	WRF	CALMET	WRF	CALMET
January	ABias	31.54	30.55	44.90	41.70	44.90	41.56
	RMSE	44.29	43.67	59.71	55.90	59.71	55.64
April	ABias	38.10	32.30	42.63	39.97	42.63	39.93
	RMSE	53.66	45.64	59.24	55.98	59.24	55.88
July	ABias	83.38	42.23	48.37	45.60	48.37	45.53
	RMSE	97.84	58.06	65.06	62.30	65.06	62.28
October	ABias	68.04	40.68	41.31	41.29	41.31	41.07
	RMSE	82.78	56.01	56.10	56.84	56.10	56.49

Table S3. The symbols and units used in this manuscript.

Symbols & Units	Meaning
WRF	the Weather Research and Forecasting model
CALMET	the meteorological diagnosing part of the air quality dispersion model CALPUFF
CALPUFF	the meteorological diagnosing part of the air quality dispersion model
$PM_{2.5}$	Particulate matter with 2.5 microns or less in diameter
LS	LaoShan
YZR	the Yangtze River
PK	Pukou District
GL	Gulou District
HGY	Jiangbei Chemical Industry Park
QX	Qixia District
LH	Liuhe District
LU	landuse use types
RMSE	root mean square error
Abias	Absolute bias
PBL	Planetary boundary layer
km	kilometer
m	meter
°	degree
hPa	hectopascal
m/s	meter per second
K	Kelvin
s^{-1}	once per second
%	percent
ton	ton
$\mu g/m^3$	microgram per cubic meter